Available online at www.sciencedirect.com
SCIENCE DIRECT®
Quaternary International 136 (2005) 15–23

CO_2/H_2O and orbitally driven climate variability over central Asia through the Holocene

Andrew B.G. Bush*

Department of Earth and Atmospheric Sciences, 126 Earth Sciences Building, University of Alberta, Edmonton, Alberta, Canada, T6G 2E3

Available online 19 January 2005

Abstract

Small variations in Earth's orbit have a direct impact on global climate with the greatest changes occurring over large land masses such as Asia. Orbitally driven climate signals are therefore likely to be identifiable in climate proxy records derived from sediment sections in the continental interior. Proxy records derived from temperature-dependent variables are also likely to display a signal due to temporal variability of atmospheric CO_2 and related climatic parameters such as water vapour content. To determine the magnitude of climate anomalies associated with shortwave and longwave radiative forcing over Asia, a suite of numerical atmospheric simulations is performed that spans most of the Holocene (from 10,000 to 2500 years BP) at 500-year intervals.

Over central Asia, the amplitude of the summer–winter seasonal cycle is greater than today in all simulations but exhibits two distinct maxima at 9000 and 6000 BP. Simulated precipitation and snow accumulation over central Asia are markedly higher during the early mid Holocene and are oscillatory, exhibiting peaks at 8000–7500 and 4500 BP (the Atlantic and Subboreal times, respectively). CO_2/H_2O forcing and orbital forcing combine to drive temperature oscillations over central Asia which, in turn, regulate relative humidity and changes in surface hydrology. Correlation between simulated results and proxy records from across Asia suggest that CO_2/H_2O and orbital forcing are dominant factors driving fluctuations of large-scale, central Asian climate through the Holocene.

1. Introduction

The geometric configuration of Earth in its orbit about the Sun, as fully determined by the three orbital parameters of obliquity, eccentricity, and longitude of perihelion (Berger, 1992), prescribes the latitudinal and seasonal distribution of incoming solar radiation (insolation) at the "top" of Earth's atmosphere. The energy transmitted by this insolation, integrated over the cross-sectional area of the Earth (including its atmosphere) determines the net amount of incoming energy available for all processes in the climate system.

It is therefore obvious that any factors that change either the magnitude or the spatio-temporal distribution of insolation have a direct impact on climate. Factors that change the net magnitude of received insolation are distance from the Sun (which varies seasonally), solar cycles in sunspot activity of 11 and 22 years (e.g., Russell and Mulligan, 1995), solar variability on geologic timescales (e.g., Endal, 1981), as well as any material (e.g., interplanetary dust particles) that passes between the Sun and the Earth and interacts with solar radiation (e.g., Kortenkamp and Dermott, 1998). Factors that directly alter the latitudinal–temporal distribution of absorbed insolation at the surface are the values of Earth's orbital parameters (Berger and Loutre, 1991; Berger, 1992), the spatial distribution of snow, ice, clouds, atmospheric water vapour, vegetation, and the temporally changing shape of the solid Earth itself (Forte and Mitrovica, 1997).

Despite the complexity and number of factors that influence the amount of insolation absorbed at the Earth's surface, there are numerous examples of paleoclimate variability that are likely to be the fingerprints of simple orbital forcing. Some examples

*Tel.: +1 780 492 3265; fax: +1 780 492 2030.
E-mail address: andrew.bush@ualberta.ca (A.B.G. Bush).

1040-6182/$ - see front matter © 2004 Elsevier Ltd and INQUA. All rights reserved.
doi:10.1016/j.quaint.2004.11.004

are: changes in strength of seasonal climate phenomena such as the south Asian monsoon (e.g., Kutzbach and Otto-Bliesner, 1982; Kutzbach and Street-Perrott, 1985; Prell and Kutzbach, 1992); sea surface temperatures in the North Atlantic (Ruddiman and McIntyre, 1984); glacial cycles (e.g., Berger et al., 1984; Colman et al., 1995; Williams et al., 1997), and; loess-paleosol sequences from the Asian interior (e.g., Rutter, 1992; Sun et al., 1999; Lu et al., 1999; Lu and Sun, 2000; Porter and An, 1995; Guo et al., 1998; Rokosh et al., 2003; Bush et al., 2004).

Of particular relevance to Holocene climate and to the present study is the ~41,000 year oscillation of Earth's angle of obliquity between approximately 24.4° and 22° (although the maximum and minimum values change within each cycle; Berger, 1992). Increased obliquity alters the seasonal distribution of insolation such that the amplitude of the seasonal cycle is enhanced. This effect is greatest at high latitudes. The value of obliquity does not in itself alter the net top-of-atmosphere incoming radiation averaged over 1 year. However, an increase in areal extent of snow and ice during high obliquity winters can produce a net deficit in annual mean insolation. Land masses in high latitudes, such as North America and Asia, are therefore particularly susceptible to climate change forced by the obliquity cycle.

Precessional effects (as described by the longitude of perihelion; Berger, 1992) become important during the early mid Holocene because they place perihelion in the boreal summertime. This effect should be particularly important during the summer months of June–July–August (JJA; see Kutzbach and Otto-Bliesner, 1982) and its effect should be maximized in the continental interior of large northern hemisphere landmasses.

In addition, there were variations of atmospheric carbon dioxide through the Holocene (Indermühle et al., 1999). These variations have the potential to amplify or mute climatic signals associated strictly with orbital forcing. However, fluctuations in atmospheric carbon dioxide also change the hydrological cycle and the amount of water vapour in the atmosphere. This in turn changes surface hydrology and the surface biosphere, which then alters the carbon flux from the surface, creating a CO_2/H_2O feedback.

As a step towards unravelling the complexities of the Asian climate record, we examine solely the combined effect of orbital and CO_2/H_2O forcing on Holocene climate over Asia using an atmospheric general circulation model (GCM) to simulate the climate from 10,000 calendar years before present (BP) to 2500 BP at 500-year intervals. These time-slice simulations therefore span approximately half of the Boreal, all of the Atlantic, and all of the Subboreal periods (using terminology from the modified Blytt–Sernander sequence as defined in Mangerud et al., 1974).

The next section discusses the model used to perform the simulations as well as the simplifying assumptions made in these sensitivity experiments. Results are then presented, followed by a discussion and concluding remarks.

2. The model

Data are generated by an atmospheric general circulation model (Gordon and Stern, 1982). All simulations are 20 years in duration and include the seasonal cycle.

The experiments are sensitivity tests designed to focus on the combined effect of orbital forcing and CO_2/H_2O forcing. We therefore fix other complicating parameters such as sea surface temperature (SST), sea level, and land surface vegetation. Modern global sea surface temperatures are therefore specified according to Levitus (1982). Although orbital forcing clearly affects the oceans in high latitudes (e.g., Ruddiman and McIntyre, 1984) as well as in the tropics (e.g., Clement et al., 1999) and can potentially be dominated by tropical SST forcing in certain regions (Bush, 2001), experiments with specified SST are chosen in order to focus more cleanly on the radiative forcing in a region relatively remote from oceanic influence. Note that, in the model, temporally varying CO_2 partially compensates for the lack of SST variability since marine processes were in part responsible for the changes in CO_2 (along with land surface change; Indermühle et al., 1999). Although we assume modern SST for consistency between these sensitivity tests, we do not imply that SST is likely to have been similar to todays throughout the Holocene.

Similarly, we assume for consistency that the land surface is the same in all simulations. Although unrealistic for the Asian interior (e.g., Khotinsky, 1984; Tarasov et al., 1997; Tarasov et al., 2000) this assumption significantly simplifies interpretation of the results and eliminates the complicating vegetation/CO_2/H_2O feedback. Note, however, that this feedback is to some degree captured by the temporally varying CO_2 concentrations, which were determined in part by changes in land cover and SST (Indermühle et al., 1999). It would therefore be inconsistent to prescribe these values of CO_2 and include dynamic vegetation. Bare land surface albedos are therefore fixed at modern values (although they can be changed by snowfall). Since the value of CO_2 is prescribed, changes in water vapour content are a direct result of combined orbital and CO_2 forcing, and the important but complex issue of secondary feedbacks on atmospheric CO_2 levels (e.g., Ruddiman, 2004) is eliminated.

The atmospheric model is a spectral one with 30 waves included in the rhomboidal truncation scheme. This produces an equivalent spatial resolution of 3.75°

in longitude and 2.25° in latitude at the equator. In the early Holocene simulations, we include the lingering remnants of the Laurentide and Fennoscandian ice sheets since they impact net insolation, and assign to them a bare ice albedo of 0.6 (which is the value assigned to Greenland and Antarctica in simulations of today). Ice sheet areal extent and topographic height were specified according to the ICE-4G reconstructions of Peltier (1994). For time slices that fall between those for which there are ice sheet reconstructions, we linearly interpolate the ice sheet data.

Soil moisture is computed using a bucket scheme with a 15 cm capacity. Modelled values of soil moisture are useful indicators of drier or wetter conditions since its computation involves all hydrological parameters.

Monthly data have been temporally averaged over the 20 years of integration. The question of how radiative changes affect the climate of a relatively large geographic region (central Asia) is most easily addressed and interpreted by examining spatially averaged quantities. Results to be shown have therefore been spatially averaged over the area shown in Fig. 1. In modern climate this area is predominantly a type-D climate zone in the Köppen classification scheme. This procedure has the advantage that it smoothes over the spatial variability in the region, thereby increasing the statistical significance of the results (see next section). We do not address here the issue of spatial variability of climate change across the Asian interior, although the reader is referred to Bush et al. (2004) for some discussion of the variability of model results and their relation to the enormously complex proxy data.

Atmospheric carbon dioxide is prescribed by data from Taylor Dome (Indermühle et al., 1999) and exhibits a decrease from the Boreal (10,000–9000 BP) to a distinct minimum at 8000 BP (early Atlantic) followed by a relatively rapid rise in the late Atlantic, and a slower rise through the Subboreal (Fig. 2A). Also shown are the values of obliquity, eccentricity, and longitude of perihelion in the simulations (Figs. 2B–D, respectively). Obliquity decreases gradually and monotonically from its Boreal maximum to today (Fig. 2B), while Earth's orbit becomes more circular (Fig. 2C).

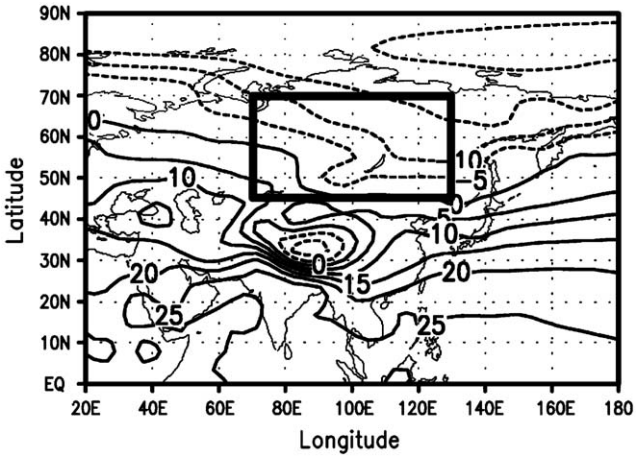

Fig. 1. The inset box indicates the area over which all model results are averaged (75°E–130°E; 45°N–70°N). Contours are mean annual temperature in the modern control simulation (0 kYr BP), in degrees Centigrade (contour interval 5 °C).

Since CO_2 and water vapour are inextricably linked in the model, we henceforth refer to CO_2/H_2O forcing as the combined effect of changes in these trace gases. Note, however, that since the feedback of H_2O on CO_2 has been eliminated in the model by specifying the land surface and SST, any changes in atmospheric water vapour is considered to be a secondary forcing. For clarity, however, we refer to the combined effect as CO_2/H_2O forcing. Simulated climate changes are therefore attributable to either carbon dioxide forcing (in conjunction with a secondary H_2O effect) or orbital forcing (although we note that in the early Holocene simulations the remnants of the Laurentide ice sheet should decrease global temperature to some degree since net insolation is reduced). A control simulation (marked as 0 kYr BP in the following figures) is performed for today's climate.

Since orbital parameters are computed according to calendar years many of the continental proxy records are in radiocarbon years, we show in all histogram figures both calendar years and the modified Blytt–Sernander sequence (Mangerud et al., 1974) for which the uncorrected radiocarbon year boundaries have been corrected to calendar years in a manner consistent with the work of Stuiver et al. (1998).

3. Results

Simulated annual mean temperature over central Asia is colder than today during the Boreal and early Atlantic, and increases relatively rapidly in the mid–late Atlantic (Fig. 2E). Warmest temperatures, however, occur in the mid–late Subboreal (3500–3000 BP). In general, the warming trend is congruent with the increase in atmospheric CO_2. However, the oscillatory nature of surface temperature (i.e. local maxima at 8000 , 5500 , and 3000 BP) cannot be explained by the levels of CO_2/H_2O. [In Fig. 2E and all subsequent plots of annual mean quantities are included lines marking the 99%, 95%, and 75% levels of statistical significance as determined by a Student T-test (using a mean variance to translate the statistical T value into a numeric value for the plotted variable; seasonal values (not shown) are comparable). The simulated mid–late Atlantic warming is therefore highly significant.]

A seasonal breakdown into JJA (Fig. 2F) and December–January–February (DJF; Fig. 2G) temperatures reveals that the increase in seasonal cycle

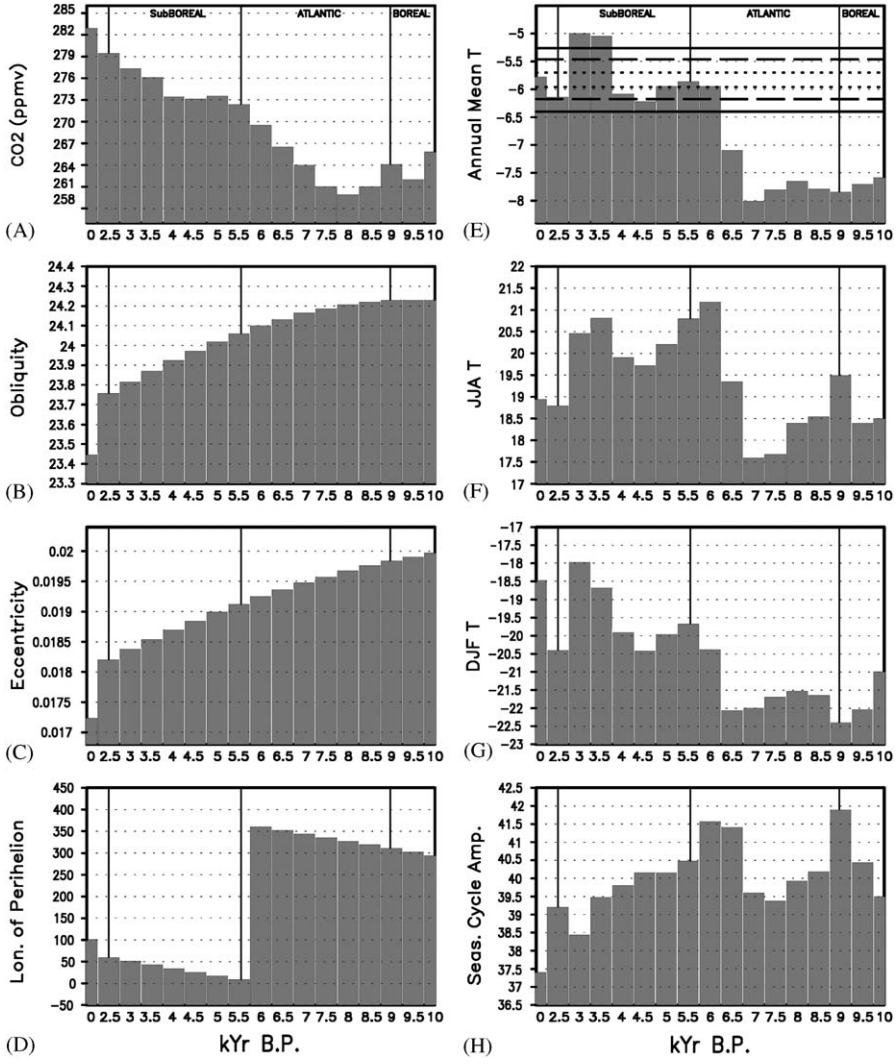

Fig. 2. (A) Atmospheric carbon dioxide (parts per million by volume) used in the simulations (data from Indermühle et al. (1999)). Values of (B) obliquity, (C) eccentricity, and (D) longitude of perihelion are from Berger (1992). Data in the histograms (E)–(H) have been spatially averaged over the area shown in Fig. 1 (see text for details). (E) Annual mean temperature in all experiments. In this and all other figures, the simulations are referred to by their calendar year BP (in thousands of years) on the *x*-axis. The control simulation is therefore "0"; (F) JJA mean temperature; (G) DJF mean temperature, and (H) amplitude of the seasonal cycle, defined as the JJA minus DJF temperature. All units are degrees Centigrade. Periods of the Blytt–Sernander sequence are marked in the top panel, with vertical lines marking the approximate boundaries in all panels. Horizontal lines in the annual mean panels (A, B, E, and H) indicate statistical significance levels according to the Student *T*-test at the 99% (solid), 95% (dashed), and 75% (dotted) levels (see text for details).

amplitude (Fig. 2H) is, from 10,000 to 6500 BP, a result of colder winters rather than warmer summers.

In the early to mid-Holocene, CO_2 is relatively low and should, all else being equal, depress both summer and winter mean temperatures compared to today. In addition, however, high values of obliquity in the early mid Holocene (cf. Fig. 2B) produce warmer summers and colder winters (i.e. an increase in seasonal cycle amplitude). This is most apparent at 9000 BP, when high obliquity dominates and produces the coldest winter and warmest summer of the early Holocene (Figs. 2F–H). In terms of temperature, the net result of CO_2/H_2O and orbital forcing in the early Holocene is that the change in the winter season is greater than that in the summer season. In addition, central Asia is subject to seasonal snow cover. There is therefore a snow-albedo feedback embedded within the annual mean temperature change. The snow-albedo feedback, combined with CO_2/H_2O forcing, introduces an asymmetry to obliquity-driven temperature change and shifts simulated annual mean temperatures towards colder values in the early mid Holocene when snow accumulation is particularly high in the Asian interior (Fig. 3A). The oscillatory nature of wintertime snow accumulation, with relative maxima in the late Boreal, the mid-Atlantic, the mid-Subboreal, and the late Subboreal, correlates with simulated annual (and seasonal) soil moisture levels (Figs. 3B–D). In our simulations, it also correlates with annual mean (and

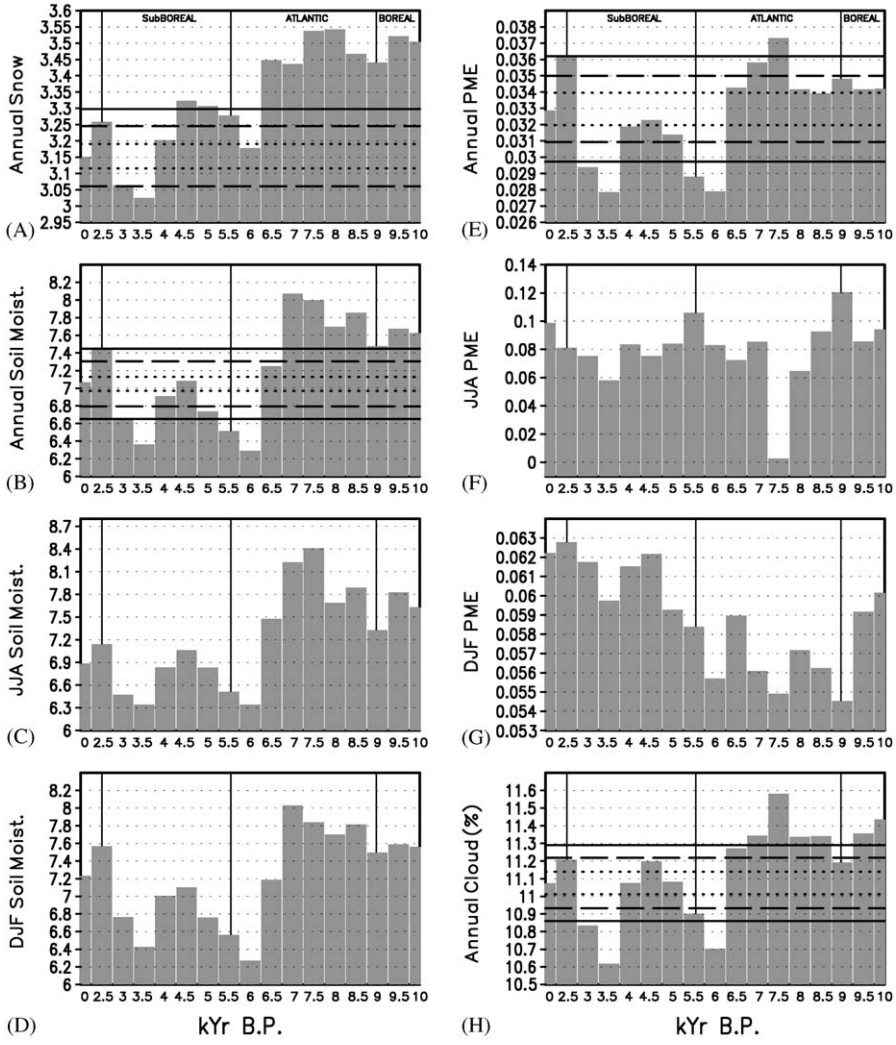

Fig. 3. (A) Annual mean snow accumulation in units of centimeters of water equivalent. (B) Annual mean soil moisture in units of centimeters. A value of 15 is completely saturated soil. (C) JJA soil moisture. (D) DJF soil moisture. (E) Annual mean freshwater flux (precipitation minus evaporation) in units of cm/day. (F) JJA freshwater flux. (G) DJF freshwater flux. (H) Annual mean cloud cover, in percent, vertically averaged over all model levels. All data are spatially averaged over the region shown in Fig. 1.

summertime) freshwater flux (precipitation minus evaporation; Figs. 3E–G) and annual mean cloud cover (Fig. 3H).

Fluctuations of precipitation in summer (rain) and winter (snow) are ultimately governed by fluctuations of relative humidity (Figs. 4A–C), whose values govern the occurrence of precipitation events. In the Boreal and mid-Atlantic, simulated relative humidity values are generally higher than today (with the exception of 9000 BP) but drop during the late-Atlantic to a minimum at 6000 BP. This pattern is inversely related to the changes in temperature (cf. Fig. 2E). This result indicates that the exponential dependence of saturation vapour pressure on temperature (e.g., Peixoto and Oort, 1992) dominates any change in water vapour pressure itself (as inferred from changes in the mixing ratio; Fig. 4D). For example, although the early Holocene is colder than today (Fig. 2E) and there is less water vapour in the air (Fig. 4D), it is relatively more humid (Fig. 4A) because of the exponential decrease of saturation vapour pressure with temperature. As a result, cloud formation increases (Fig. 3H) and more precipitation occurs (Fig. 3E).

The degree of correlation between model variables is not surprising given the fact that orbital and CO_2 changes affect temperature, which directly affects saturation vapour pressure, atmospheric water vapour content (Fig. 4D), and relative humidity (Fig. 4A). Relative humidity, in turn, regulates saturation events such as cloud formation (Fig. 3H), precipitation (Fig. 3E), snowfall (Fig. 3A) and soil moisture (Fig. 3B).

From 10,000 to 6500 BP the simulations therefore suggest colder and wetter conditions, with a transition to warmer and drier conditions from 6500 to 5500 BP. Embedded within this early to mid-Holocene change, however, are more rapid oscillations that cannot be

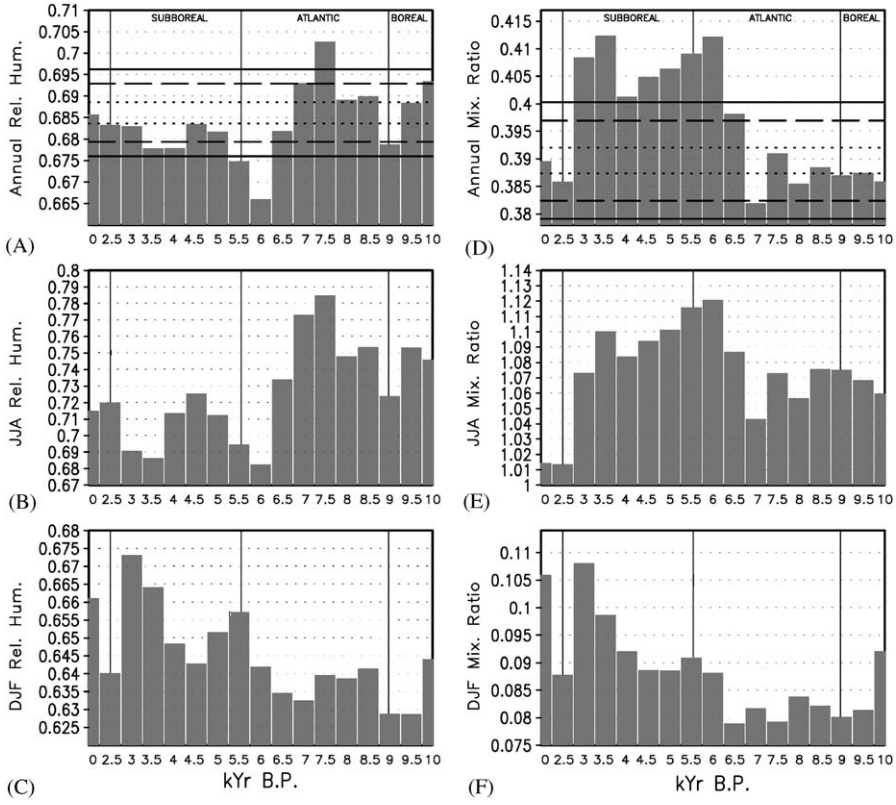

Fig. 4. (A) Annual mean relative humidity (multiply by 100 for percent). (B) JJA relative humidity. (C) DJF relative humidity. (D) Annual mean mixing ratio. (E) JJA mixing ratio. (F) DJF mixing ratio. Units in (D)–(F) are grams of water vapour per gram of dry air, multiplied by 100.

explained by the CO_2/H_2O forcing (cf. Fig. 2A). For example, moisture variables (e.g., snow, soil moisture) show a relative maximum in the early mid Subboreal (~4500 BP) when annual mean temperature has a relative minimum (cf. Fig. 2E) but CO_2 is relatively constant. Similarly in the late Subboreal (~3500–3000 BP), when the increase in CO_2 is relatively slight, there is a relative maximum of temperature and relative minima in snow, freshwater flux, and cloud amount.

4. Discussion

The impact of Holocene CO_2/H_2O forcing on the climate of central Asia is indicated by the general trend toward warmer temperatures from the early to the mid-Holocene. In the late Boreal/early Atlantic (9000 BP), however, there is a decoupling of CO_2/H_2O and temperature such that slightly higher CO_2 levels (Fig. 2A) are coincident with cooler annual mean temperature (Fig. 2E) and reduced soil moisture (Figs. 3B). The reduced surface hydrology at this time is caused by the dominance of colder winter temperatures over warmer summer temperatures (Figs. 2F and G) and significantly reduced winter precipitation (Fig. 3G). This wintertime dominance occurs at a time when the seasonal cycle amplitude is at its greatest value of the Holocene (Fig. 2H) and indicates that orbital forcing dominates CO_2/H_2O forcing at this time. From proxy data, this time also correlates with late Boreal cooling in northern Eurasia, western Europe, and North America (Khotinsky, 1984).

Increasing temperatures in the Atlantic (Fig. 2E) are coincident with the rise in atmospheric CO_2/H_2O (Figs. 2A, 4D) and show the greatest increase in the late Atlantic (6500–6000 BP). This trend is consistent with the expansion of forest across Asia, which is also most evident in the late Atlantic (Khotinsky, 1984). The seasonal cycle amplitude in the late Atlantic is much greater than today and its maximum value (at 6000 BP) is nearly as large as at 9000 BP. The Atlantic is therefore characterized by relatively cool and humid conditions for the first 2000 years, followed by warmer and less humid conditions for the next 1300 years. The Atlantic rise in water vapour content (Fig. 4D) is anticorrelated with precipitation amounts and soil moisture (Figs. 3A, B, E). This result is consistent with the temperature increase and its consequent increase of the saturation vapour pressure. These results appear to be consistent with the reconstruction of Khotinsky (1989; see discussion in Karabanov et al., 2000). Data from the Chinese Loess Plateau also indicate a cooler, moister early

Holocene climate followed by a warmer, more arid climate in the mid-Holocene (e.g., Liu et al., 2002; Chen et al., 2003; Tarasov et al., 2000).

In the early Subboreal (from 5500 to 4500 BP), however, there is a cooling trend that does not appear to be driven by the relatively constant levels of carbon dioxide (Figs. 2A and E). (Despite the fact that annual mean temperatures at 5500 BP are statistically similar to today's, the temperatures at 4500 BP are cooler than today at 95% significance level so this cooling trend is statistically significant.) Early Subboreal cooling is primarily caused by a reduction of summertime temperatures (Fig. 2F) that drives an increase in relative humidity in an atmosphere that has a relatively high amount of water vapour (Figs. 4A and D). This period would therefore be characterized by relatively cool and wet conditions.

The transition to mid-Subboreal (4500–3000 BP) shows warmer (Fig. 2E) and drier (Figs. 3A,B,E) annual mean conditions followed by late Subboreal (3000–2500 BP) cooling and wetting. The magnitude of the mid-Subboreal warming, in particular, cannot be wholly explained by CO_2/H_2O levels and must therefore contain an orbital component. From palynologic data, the Subboreal period has been subdivided into three phases as follows (Khotinsky, 1984). The first (4600–4100 radiocarbon years, which approximately equals 5500–4600 BP) was characterized by cooling and a southward expansion of tundra. The second (4100–3200 radiocarbon years, or ~4600–3500 BP) was characterized by warming and a northward retreat of tundra with an expansion of forest. The third (3200–2500 radiocarbon years, or ~3500–2600 BP) was characterized by cooling and a southward migration of the forest/tundra line. Model results of annual temperature (Fig. 2E) are therefore in excellent agreement with the temperature trends interpreted from the proxy data. In addition, the warming simulated for the mid-Subboreal is of a relatively large magnitude (second only to the late Atlantic warming; cf. Fig. 2E) and this is also seen in the data from northern European Russia (Khotinsky, 1984). Orbital control of climate therefore appears to be more important than CO_2/H_2O forcing during this time period.

From these simulations we therefore suggest that the Boreal/Atlantic cooling, the early mid-Atlantic warming, the early Subboreal cooling, the mid-Subboreal warming, and the late Subboreal cooling are driven by orbital forcing since they are contrary to what would be expected from the prescribed CO_2 forcing. We also suggest that the mid–late Atlantic warming, which is the dominant trend of the Holocene, is primarily driven by CO_2/H_2O (Figs. 2A, 4D).

The general agreement between these model results and the paleoreconstructions for climate over central Asia is encouraging. For example, the significant mid–late Atlantic warming is seen throughout Eurasia (Khotinsky, 1984). Also, the high simulated annual temperature during the Subboreal may have support in the diatom record of Lake Baikal (Karabanov et al., 2000), and the subsequent cooling and drying appears to have occurred across the entire Asian interior (e.g., Starkel, 1998). Simulated increases in the hydrological cycle are in broad agreement with greater lake levels in the early Holocene (Harrison et al., 1996; Bernasconi et al., 1997; Lehmkuhl and Lang, 2001) and reduced mid-Holocene lake levels in regions remote from the Asian monsoon (Qin and Yu, 1998).

From the model results, two time slices exhibit anomalous climates that may warrant further examination of proxy data: the mid-Atlantic (7000 BP), which should exhibit vegetation consistent with cold and wet conditions (both in summer and winter); and the late Subboreal (2500 BP), which should also exhibit species that prefer wet conditions (in both summer and winter). The broad agreement between model results and proxy records implies that, for this region of the world during this time period, oceanic and land surface influences are comparatively small. Of course, when large global events such as glaciations or Dansgaard-Oeschger/Bond cycles occur they are recorded in, for example, the sediments of Lake Baikal (Williams et al., 1997; Khursevich et al., 2001; Prokopenko et al., 2001). Our results suggest that in the absence of such extreme global events, climatic oscillations associated with orbital and CO_2/H_2O forcing over central Asia were sufficiently large that they would have affected ecosystems across the entire Asian interior.

On a final note, anthropological evidence for a cultural replacement of people in the Lake Baikal region during the late Atlantic (Weber et al., 2002) naturally raises the intriguing question of whether the largest and most rapid climate change of the Holocene, as simulated here, may have had a direct influence on human evolution in the Asian interior. This fundamental question will be the subject of future work.

5. Conclusions

Simulations of Holocene air temperature and hydrological cycle variables from a general circulation model show a high degree of temporal climate variability during the Holocene in the region of central Asia. This variability is driven by a combination of CO_2/H_2O and orbital forcing. Warming over central Asia in the mid–late Atlantic period is driven primarily by CO_2/H_2O forcing, whereas other climate fluctuations in the late Boreal, the early mid-Atlantic, and throughout the Subboreal, are driven primarily by orbital forcing. Since simulated results are in general agreement with some of the paleoreconstructions of Asian climate from

palynological data we can conclude that the specific forcing factors examined here are the dominant mechanisms controlling climate variability over central Asia, and that each factor was dominant at different times through the Holocene.

Acknowledgements

The author thanks the reviewers of a previous version of this work; your comments helped enormously and were appreciated. The author gratefully acknowledges funding from the Canadian Natural Sciences and Engineering Council (G121210769) and participation in the Earth System Evolution Program of the Canadian Institute for Advanced Studies (CIAR).

References

Berger, A., 1992. Orbital variations and insolation database. IGBP PAGES/World Data Center-A for Paleoclimatology Data Contribution Series # 92-007. NOAA/NGDC Paleoclimatology Program, Boulder, CO, USA.

Berger, A., Loutre, M.F., 1991. Insolation values for the climate of the last 10 million years. Quaternary Sciences Reviews 10, 297–317.

Berger, A.L., Imbrie, J., Hays, J., Kukla, G., Saltzman, B., 1984. Milankovitch & Climate. D. Reidal, Dordrecht, Netherlands.

Bernasconi, S.M., Dobson, J., McKenzie, J.A., Ariztegui, D., Niessen, F., Hsu, K.J., Chen, Y., Yang, Q., 1997. Preliminary isotopic and palaeomagnetic evidence for Younger Dryas and Holocene climate evolution in NE Asia. Terra Nova 9, 246–250.

Bush, A.B.G., 2001. Pacific sea surface temperature forcing dominates orbital forcing of the early Holocene monsoon. Quaternary Research 55, 25–32.

Bush, A.B.G., Little, E.C., Rokosh, D., White, D., Rutter, N.W., 2004. Climatic interpretation of Late Quaternary loess-paleosol sequences from across the Asian interior. Quaternary Science Reviews 23, 481–498.

Chen, C.-T.A., Lan, H.-C., Lou, J.-Y., Chen, Y.-C., 2003. The dry Holocene Megathermal in Inner Mongolia. Palaeogeography, Palaeoclimatology, Palaeoecology 193, 181–200.

Clement, A.C., Seager, R., Cane, M.A., 1999. Orbital controls on the El Niño/Southern Oscillation and the tropical climate. Paleoceanography 14, 441–456.

Colman, S.M., Peck, J.A., Karabanov, E.B., Carter, S.J., Bradbury, J.P., King, J.W., Williams, D.F., 1995. Continental climate response to orbital forcing from biogenic silica records in Lake Baikal. Nature 378, 769–771.

Endal, A.S., 1981. Evolutionary variations of solar luminosity. In: Variations of the Solar Constant. NASA Conference Publication 2191, pp. 175–183.

Forte, A.M., Mitrovica, J.X., 1997. A resonance in Earth's obliquity and precession over the past 20 Myr driven by mantle convection. Nature 390, 676–680.

Gordon, C.T., Stern, W., 1982. A description of the GFDL global spectral model. Monthly Weather Review 110, 625–644.

Guo, Z.T., Liu, T.S., Fedoroff, N., Wei, L.Y., Ding, Z.L., Wu, N.Q., Lu, H.Y., Jian, W.Y., An, Z.S., 1998. Climate extremes in loess of China coupled with the strength of deep-water formation in the North Atlantic. Global and Planetary Change 18, 113–128.

Harrison, S.P., Yu, G., Tarasov, P.E., 1996. Late Quaternary lake-level record from northern Eurasia. Quaternary Research 45, 138–159.

Indermühle, A., Stocker, T.F., Joos, F., Fischer, H., Smith, H.J., Wahlen, M., Deck, B., Mastroianni, D., Tschumi, J., Blunier, T., Meyer, R., Stauffer, B., 1999. Holocene carbon-cycle dynamics based on CO_2 trapped in ice at Taylor Dome, Antarctica. Nature 398, 121–126.

Karabanov, E.B., Prokopenko, A.A., Williams, D.F., Khursevich, G.K., 2000. A new record of Holocene climate change from the bottom sediments of Lake Baikal. Palaeogeography, Palaeoclimatology, Palaeoecology 156, 211–224.

Khotinsky, N.A., 1984. Holocene climate change. In: Velichko, A.A. (Ed.), Late Quaternary Environments of the Soviet Union. University of Minnesota Press, Minneapolis, pp. 305–309.

Khotinsky, N.A., 1989. Discussion of problems of Holocene correlation and paleoreconstructions. In: Khotinsky, N.A. (Ed.), Paleoclimates of the Last Glacial and the Holocene. Nauka, Moscow, pp. 12–14 (in Russian).

Khursevich, G.K., Karabanov, E.B., Prokopenko, A.A., Williams, D.F., Kuzmin, M.I., Fedenya, S.A., Gvozdkov, A.A., 2001. Insolation regime in Sibera as a major factor controlling diatom production in Lake Baikal during the past 800,000 years. Quaternary International 80–81, 47–58.

Kortenkamp, S.J., Dermott, S.F., 1998. A 100,000-year periodicity in the accretion rate of interplanetary dust. Science 280, 874–876.

Kutzbach, J.E., Otto-Bliesner, B.L., 1982. The sensitivity of the African–Asian monsoonal climate to orbital parameter changes for 9000 years B.P. in a low-resolution general circulation model. Journal of Atmospheric Science 39, 1177–1188.

Kutzbach, J.E., Street-Perrott, F.A., 1985. Milankovitch forcing of fluctuations in the level of tropical lakes from 18 to 0 kyr BP. Nature 317, 130–134.

Lehmkuhl, F., Lang, A., 2001. Geomorphological investigations and luminescence dating in the southern part of the Khangay and the valley of the Gobi Lakes (Central Mongolia). Journal of Quaternary Science 16, 69–87.

Levitus, S., 1982. Climatological atlas of the world ocean. NOAA Prof. Paper 13, US Government Printing Office, Washington, DC, 173pp.

Liu, H., Xu, L., Cui, H., 2002. Holocene history of desertification along the woodland-steppe border in Northern China. Quaternary Research 57, 259–270.

Lu, H.Y., Sun, D.H., 2000. Pathways of dust input to the Chinese Loess Plateau during the last glacial and interglacial periods. Catena 40, 251–261.

Lu, H.Y., VanHuissteden, K.O., An, Z.S., Nugteren, G., Vandenberghe, J., 1999. East Asia winter monsoon variations on a millennial time-scale before the last glacial–interglacial cycle. Journal of Quaternary Science 14, 101–110.

Mangerud, J., Andersen, S.T., Berglund, B.E., Donner, J.J., 1974. Quaternary stratigraphy of Norden, a proposal for terminology and classification. Boreas 3, 109–128.

Peixoto, J.P., Oort, A.H., 1992. Physics of Climate. American Institute of Physics, New York 520pp.

Peltier, W.R., 1994. Ice age paleotopography. Science 265, 195–201.

Porter, S.C., An, Z.S., 1995. Correlation between climate events in the North Atlantic and China during last glaciation. Nature 375, 305–308.

Prell, W.L., Kutzbach, J.E., 1992. Sensitivity of the Indian monsoon to forcing parameters and implications for its evolution. Nature 360, 647–652.

Prokopenko, A.A., Karabanov, E.B., Williams, D.F., Kuzmin, M.I., Khursevich, G.K., Gvozdkov, A.A., 2001. The detailed record of climatic events during the past 75,000 yrs BP from the Lake Baikal drill core BDP-93-2. Quaternary International 80-81, 59–68.

Qin, B.Q., Yu, G., 1998. Implications of lake level variations at 6 and 18 ka in mainland Asia. Global and Planetary Change 18, 59–72.

Rokosh, D., Bush, A.B.G., Rutter, N.W., Ding, Z., Sun, J., 2003. Hydrologic and geologic factors that influenced spatial variations in loess deposition in China during the last interglacial–glacial cycle: results from proxy climate and GCM analyses. Palaeogeography, Palaeoclimatology, Palaeoecology 193, 249–260.

Ruddiman, W.F., 2004. The role of greenhouse gases in orbital-scale climatic changes. EOS 85, 1,6–7.

Ruddiman, W.F., McIntyre, A., 1984. Ice-age thermal reponse and climatic role of the surface Atlantic Ocean, 40°N to 63°N. Geological Society of America Bulletin 95, 381–396.

Russell, C.T., Mulligan, T., 1995. The 22-year variation of geomagnetic activity: implications for the polar magnetic field of the sun. Geophysical Research Letters 22, 3287–3288.

Rutter, N.W., 1992. Presidential Address, XIII INQUA Congress 1991: Chinese loess and global change. Quaternary Science Reviews 11, 275–281.

Starkel, L., 1998. Geomorphic response to climatic and environmental changes along a Central Asian transect during the Holocene. Geomorphology 23, 293–305.

Stuiver, M., Reimer, P.J., Bard, E., Beck, J.W., Burr, G.S., Hughen, K.A., Krmoer, B., McCormac, F.G., v.d. Plicht, J., Spurk, M., 1998. INTCAL98 radiocarbon age calibration 24,000–0 cal BP. Radiocarbon 40, 1041–1083.

Sun, J.M., Ding, Z.L., Liu, T.S., Rokosh, D., Rutter, N.W., 1999. 580,000-year environmental reconstruction from aeolian deposits at the Mu Us desert margin, China. Quaternary Science Reviews 18, 1351–1364.

Tarasov, P.E., Jolly, D., Kaplan, J.O., 1997. A continuous Late Glacial and Holocene record of vegetation changes in Kazakhstan. Palaeogeography, Palaeoclimatology, Palaeoecology 136, 281–292.

Tarasov, P., Dorofeyuk, N., Metel'Tseva, E., 2000. Holocene vegetation and climate changes in Hoton-Nur Basin, northwest Mongolia. Boreas 29, 117–126.

Weber, A.W., Link, D.W., Katzenberg, M.A., 2002. Hunter–gatherer culture change and continuity in the middle Holocene of the Cis-Baikal, Siberia. Journal of Anthropological Archaeology 21, 233–299.

Williams, D.F., Peck, J., Karabanov, E.B., Prokopenko, A.A., Kravchinsky, V., King, J., Kuzmin, M.I., 1997. Lake Baikal record of continental climate response to orbital insolation during the past 5 million years. Science 278, 1114–1117.